



1 **Chemical composition and light absorption of carbonaceous aerosols**
2 **emitted from crop residue burning: Influence of combustion**
3 **efficiency**

4 Yujue Wang,¹ Min Hu,^{*,1,2,4} Nan Xu,¹ Yanhong Qin,¹ Zhijun Wu,^{1,2} Liwu Zeng,³ Xiaofeng Huang,³
5 Lingyan He³

6 ¹State Key Joint Laboratory of Environmental Simulation and Pollution Control, College of Environmental Sciences and
7 Engineering, Peking University, Beijing 100871, China

8 ²Collaborative Innovation Center of Atmospheric Environment and Equipment Technology, Nanjing University of
9 Information Science & Technology, Nanjing, China

10 ³Key Laboratory for Urban Habitat Environmental Science and Technology, School of Environment and Energy, Peking
11 University Shenzhen Graduate School, Shenzhen, China

12 ⁴Beijing Innovation Center for Engineering Sciences and Advanced Technology, Peking University, Beijing 100871, China

13 *Correspondence to:* Min Hu (minhu@pku.edu.cn)

14

15 **Abstract.** Biomass burning is one of the major sources of carbonaceous aerosols, which affects air quality, radiation budget
16 and human health. Field straw residue burning is a widespread type of biomass burning in Asia, while its emissions are
17 poorly understood compared with the wood burning emissions. In this study, lab-controlled straw (wheat and corn) burning
18 experiments were designed to investigate the emission factors and light absorption properties of different biomass burning
19 organic aerosol (BBOA) fractions, including water soluble organic carbon (WSOC), humic-like substances (HULIS) and
20 water insoluble organic carbon (WISOC). The influences of biofuel moisture content and combustion efficiency on
21 emissions are comprehensively discussed. The emission factors of PM_{2.5}, OC and EC were 9.3±3.4, 4.6±1.9 and 0.21±0.07
22 g/kg for corn burning and 8.7±5.0, 3.9±2.8 and 0.22±0.05 g/kg for wheat burning, generally lower than wood or forest
23 burning emissions. Though the mass contribution of WISOC among OC (32%-43%) was lower than WSOC, the light
24 absorption contribution of WISOC (57%–84% @300-400 nm) surpassed WSOC due to the higher mass absorption
25 efficiency (MAE) of WISOC. The results suggested that BBOA light absorption would be largely underestimated if only
26 considering the water soluble fractions. However, the light absorption of WSOC among near-UV ranges, occupying 39%-43%
27 of the total extracted OC absorption at 300 nm, cannot be negligible due to the sharper increase of absorption towards shorter
28 wavelength compared with WISOC. HULIS were the major light absorption contributors among WSOC, due to the higher
29 MAE of HULIS than other high-polarity WSOC components. The emission levels and light absorption of BBOA were
30 largely influenced by the burning conditions, indicated by modified combustion efficiency (MCE) calculated by measured
31 CO and CO₂ in this work. The emission factors of PM_{2.5}, OC, WSOC, HULIS and organic acids were enhanced under
32 lower-MCE conditions or during higher-moisture straw burning experiments. Light absorption coefficients of BBOA at 365



33 nm were also observed higher under lower-MCE conditions, which was mainly due to the elevated mass emission factors.
34 Our results suggested that the influence of varied combustion efficiency on particle emissions could surpass the differences
35 caused by different types of biofuels. Thus, the burning efficiency or conditions should be taken into consideration when
36 estimating the influence of biomass burning. In addition, we observed that the K^+/OC and Cl^-/OC ratios increased under
37 higher-MCE conditions due to the enhancement of released potassium and chlorine under higher fire temperatures during
38 flaming combustion. This indicates that potassium ion, as a commonly used biomass burning tracer, may lead to estimation
39 uncertainty if without considering the burning conditions.

40

41 **1 Introduction**

42 Biomass burning emissions, as a major primary source of carbonaceous aerosols, have significant effects on the air
43 quality, human health as well as regional or global radiation budget (Bond, 2004; Chen et al., 2017a; Reid et al., 2005; Saleh
44 et al., 2015). Biomass burning could contribute one-third of the black carbon (BC) budget and two-thirds of the primary
45 organic aerosol budget on the global scale (Bond, 2004; Bond et al., 2013). In recent years, biomass burning organic aerosols
46 (BBOA) also attracted much attention due to their substantial contribution to light-absorbing organic aerosols, known as
47 brown carbon (BrC) (Andreae and Gelencsár, 2006; Laskin et al., 2015; Lin et al., 2016; Saleh et al., 2014; Washenfelder et
48 al., 2015; Yan et al., 2018). Emission factors (EF) of BrC ranged from 1.0 to 1.4 g/kg biomass, comparable to those of BC
49 (Aurell and Gullett, 2013). Majority of BrC aerosol mass was associated with biomass burning emissions in rural southeast
50 US (Washenfelder et al., 2015). Regional radiative forcing effects of BrC could be comparable to those of BC over major
51 areas dominated by biomass burning and biofuel combustion, such as South and East Asia (Feng et al., 2013).

52 Emission factors, chemical compositions and light absorption properties of biomass burning aerosols could be
53 obviously influenced by different types of biomass, biofuel structures, moisture contents, and especially varied burning
54 conditions (Chen and Bond, 2010; Holder et al., 2016; Reisen et al., 2018). The emissions of particulate organics could span
55 several orders of magnitude depending on different burning conditions (Chen et al., 2017a; Jen et al., 2019). In general,
56 higher levels of particulate matters (PM) and organic aerosols were emitted during less efficient biomass burning, due to
57 prolonged incomplete or smoldering combustion (Holder et al., 2016; Jen et al., 2019; Reisen et al., 2018). Open biomass
58 burning, especially smoldering combustion, dominates the organic carbon (OC) emissions in many regions of the world on
59 an annual-average basis (Bond, 2004). The light absorption of BBOA are also largely dependent on the combustion
60 conditions (Saleh et al., 2014). The contribution of BrC to aerosol light absorption at near-UV wavelength was reported
61 higher for more smoldering combustion compared with more flaming combustion (Holder et al., 2016). The reported
62 variation trends of BBOA absorption properties as a function of combustion conditions, however, are not consistent from



63 different studies. High variability in reported emission factors and optical properties of BBOA from different burning
64 conditions complicates their treatment in climate models (Liu et al., 2014; Saleh et al., 2014), and indicates the importance of
65 further investigations on biomass burning emissions, especially the influence of burning conditions.

66 Unlike the well-understood BC, the light-absorbing OC or BrC comprise a wide range of poorly characterized organic
67 compounds, which exhibit highly variable chemical and light absorption properties (Andreae and Gelencsár, 2006; Laskin et
68 al., 2015; Lin et al., 2016; Saleh et al., 2014; Washenfelder et al., 2015; Yan et al., 2018). Previous studies have suggested
69 that methanol extracted BrC were usually more light-absorbing than water extracts for BBOA or ambient aerosols (Chen and
70 Bond, 2010; Liu et al., 2013). More than 92% of the light absorbing OC emitted from solid fuel pyrolysis could be extracted
71 by methanol, compared with 73% for water-extracted compounds (Chen and Bond, 2010). Alkaline or methanol extracted
72 OC fractions were also observed with higher mass absorption efficiency (MAE) at 365 nm than water soluble organic carbon
73 (WSOC) for residential coal combustion (Li et al., 2018). Only considering the water soluble BrC would result in
74 underestimation of BrC absorption and radiative forcing (Cheng et al., 2016; Cheng et al., 2017). Different light absorption
75 properties of organic fractions could be attributed to the varied chemical compositions and structures (Chen et al., 2016a;
76 Chen et al., 2016b; Chen et al., 2017b). However, few studies have been conducted to gain a comprehensive understanding
77 on the influence of combustion conditions on the chemical composition and light absorption of different BBOA fractions.

78 Field open burning of agriculture wastes or crop residues is a widespread type of biomass burning in Asia (IARI, 2012;
79 Bond, 2004; Streets et al., 2003b). Open crop residue burning during harvest season would result in severely adverse impacts
80 on regional air quality and human health (Chen et al., 2017a; Li et al., 2014; Lin and Yu, 2011; Streets et al., 2003a; Zhang
81 et al., 2010). The PM emission factors from agricultural waste burning range from 1.7 to 17.8 g/kg (Bond, 2004). Source
82 apportionment results showed that ~50% of carbonaceous aerosols in Beijing were associated with biomass burning, with
83 crop residue combustion as a major source (Cheng et al., 2013). Straw residue burning could contribute as high as 51% of
84 PM and 76% of OC during harvest seasons in the agriculture regions in China (Li et al., 2014). Considering the large
85 contribution of straw residue burning, the chemical compositions and light absorption properties of BBOA in Asia may
86 differ from other regions with wood burning as the major type of biomass burning. However, the understanding on field
87 straw residue burning emissions is still limited. A better characterization of the emission levels and optical properties of
88 straw burning aerosols is required to quantify their effects on air quality and regional radiation forcing in agriculture area
89 (Hungershofer et al., 2008). Laboratory simulation experiment has been suggested as a good way to study biomass burning
90 emissions due to its advantage in quantifying emission factors and controlling combustion conditions within well-defined
91 limits. In this work, a series of lab burning experiments were designed to systematically investigate the emission factors,
92 chemical compositions and light absorption properties of both water-soluble and water-insoluble carbonaceous aerosols



93 emitted from straw residue burning. The influence of biofuel moisture contents, burning conditions and combustion
94 efficiency on the BBOA emission levels and light absorption properties are comprehensively discussed.

95 **2 Methods**

96 **2.1 Simulation and sampling of biomass burning aerosols**

97 Lab-controlled burning experiments were conducted in the Laboratory of Biomass Burning Simulation at Peking
98 University Shenzhen Graduate School. The simulation system was designed and optimized on the basis of the one used in He
99 et al. (2010) (He et al., 2010), which included combustion system, dilution system, sampling system and data acquisition
100 system (Figure S1). During each experiment, about 1-2 kg biomass fuels were ignited on the combustion pan. The emitted
101 smoke was collected by the hood above the fire, and diluted by zero air (21 mol% O₂ and 79 mol % N₂) before collected on
102 filters or monitored by online instruments. Smoke aerosols were collected on both Teflon (Whatman Inc.) and quartz fiber
103 (Whatman Inc.) filters, using a PM_{2.5} cutoff with a sampling flow rate of 16.7 L/min. During each burning experiment, CO
104 and CO₂ were measured continuously by CO and CO₂ analyzers (Thermo Scientific Inc., Bremen, Germany). The burning
105 efficiency, calculated based on the online CO and CO₂ data, were monitored continuously during each experiment (Table S1).
106 The variation of fire temperatures during each experiment was also measured by a sensor above the fire (Figure S1).

107 In this study, corn and wheat, two primary grain crops in China, burning was simulated to represent the straw residue
108 burning in China. To investigate the influence of biofuel moisture contents on burning emissions, straws with different levels
109 of moisture contents were burned, including low (13%) and high (18%) levels for corn burning experiments, low (7%-9%),
110 medium (18%-22%), and high (27%-33%) levels for wheat burning experiments (Table S1). The moisture content was
111 measured by drying the biofuels in the oven at 105°C for 24 h. Straw residues with different moisture contents were
112 prepared by mixing weighted biofuels with weighted pure water in a plastic box, and shaking until the water was absorbed.
113 Each experiment condition was repeated three times. All the conducted experiment conditions as well as burning conditions
114 are summarized in Table S1.

115 **2.2 Isolation of carbonaceous aerosols**

116 The quartz fiber filters were used to extract different carbonaceous aerosol fractions, including water-insoluble organic
117 carbon (WISOC), WSOC, and carbon component of Humic-Like Substances (HULIS_C). The filter samples were firstly
118 extracted in an ultrasonic bath twice using 10, and 10 mL ultrapure water, each time for 30 min. The extracts were then
119 combined and filtered with a 0.45 μm pore size syringe filter (Gelman Sciences) to obtain the WSOC solutions. After
120 removing the WSOC fraction on filters, the WISOC fractions were then extracted in an ultrasonic bath twice using 5, and 5
121 mL methanol, each time for 30 min. The extracts then were combined and filtered using a 0.25 μm syringe filter. The HULIS



122 fraction was isolated from the WSOC solutions via solid phase extraction (SPE), with majority of low molecular weight
123 organic acids (with relatively higher polarities) and sugars removed from the water solutions. Details about the HULIS
124 extraction procedures were described in our previous paper (Wang et al., 2017). The WSOC fraction excluded HULIS was
125 named as high-polarity WSOC (WSOC-h) in this study.

126 2.3 Quantification and light absorption measurements of carbonaceous aerosols

127 The total OC abundance was analyzed by a thermal/optical carbon analyzer (Sunset Laboratory). The concentrations of
128 water soluble carbonaceous aerosol fractions, including WSOC and HULIS_C, were measured using a total organic carbon
129 (TOC) analyzer (AnalytikJena multi N/C 3100). The WISOC concentrations were obtained by minus WSOC from the total
130 OC. Light absorption of the extracted solutions (WSOC, HULIS_C and WISOC) were measured by a UV-vis spectrometer
131 (UV-1780, Shimadzu) over the wavelength range of 300-700 nm. The absorptions of WSOC and WISOC were added up to
132 represent the absorption of the total extracted OC. The absorption coefficients (Abs_{λ} , Mm^{-1}) and mass absorption efficiency
133 (MAE_{λ}) of isolated solutions at a wavelength λ were calculated as follow (Cheng et al., 2011; Cheng et al., 2016):

$$Abs_{\lambda} = (A_{\lambda} - A_{700}) \frac{V_{sol}}{V_{air} \times L} \times \ln(10)$$

$$MAE_{\lambda} = \frac{Abs_{\lambda}}{C}$$

134 where A_{λ} and A_{700} represent the measured absorbance at wavelength λ and 700 nm. V_{sol} is the volume of extracted solutions
135 and V_{air} is the volume of air sampled through the filter punch. The optical path length (L) is 1 cm in the present experiments.
136 $\ln(10)$ is used to convert from common logarithm to natural logarithm. C corresponds to the concentrations of OC, WISOC,
137 WSOC or HULIS_C fractions. It is noted that the total OC was used to represent the concentration of extracted OC, which
138 may lead to an overestimation of WISOC mass concentration and an underestimation of MAE of WISOC. The wavelength
139 dependence of light absorption is described using the Absorption Angstrom Exponent (AAE), which is calculated by a linear
140 regression fit of $\log(Abs_{\lambda})$ versus $\log(\lambda)$ in the wavelength range of 300-450 nm.

141 Water-soluble K^{+} , Cl^{-} and low molecular weight organic acids (acetic acid, formic acid, succinic acid, oxalic acid,
142 propionic acid and methanesulfonic acid) were analyzed by ion chromatograph (DIONEX, ICS2500/ICS2000), following the
143 procedures described in Guo et al. (2010) (Guo et al., 2010).



144 3 Results and discussion

145 3.1 Burning conditions and combustion efficiency

146 The burning conditions and combustion efficiency, calculated by measured CO and CO₂ concentrations, of the
147 simulation experiments are shown in Figure 1 and Table S1. Modified combustion efficiency (MCE), defined as
148 $\Delta\text{CO}_2/(\Delta\text{CO}_2+\Delta\text{CO})$, is used to indicate the burning conditions during a fire (Akagi et al., 2011; Andreae and Merlet, 2001).
149 The burning conditions in this study varied from different fires, with the MCE ranging from 0.68 to 0.88 and an average
150 value of 0.77. The amount and compositions of substances emitted from a given fire are determined to a large extent by the
151 burning conditions or the ratio of flaming to smoldering combustion, which is often expressed as “combustion efficiency”.
152 Higher MCE (>0.9) indicates more flaming combustions, and lower MCE indicates more smoldering conditions. A previous
153 study suggested that pure flaming has an MCE near 0.99, and the MCE of most smoldering combustion is around or lower
154 than 0.8 (Akagi et al., 2011). The burning experiments were generally dominated by smoldering combustions in the present
155 study.

156 The biomass fuels with lower moisture contents are generally burned more efficiently, with relatively higher MCE
157 values (Table S1), which suggested higher proportion of flaming combustion during the fire. The MCE of higher-moisture
158 biomass burning was generally lower, and prolonged smoldering combustion was observed (Figure 1, Table S1). Previous
159 lab-controlled burning experiments also reported similar phenomenon that higher fuel moistures would lower the combustion
160 efficiency, shorten flaming phase and introduce prolonged smoldering combustion (Chen et al., 2010). The relative
161 proportion of flaming versus smoldering phases can vary considerably as a function of fuel moistures and structures
162 (Andreae and Merlet, 2001).

163 Figure 1 displays variations of the monitored parameters (CO, CO₂, $\Delta\text{CO}/\Delta\text{CO}_2$ and fire temperature) during two
164 selected burning experiments (low-moisture biomass burning with MCE=0.83, and high-moisture biomass burning with
165 MCE=0.68). Different burning conditions dominate at different periods of a fire and the length of each period varied by
166 experiments (Figure 1). Actually, flaming and smoldering phases occur simultaneously during a fire and the proportions of
167 different combustion types vary over time (Akagi et al., 2011; Andreae and Merlet, 2001). For example, the initial period of
168 low-moisture biomass burning experiment (Figure 1a) is dominated by flaming, wherein CO₂ increased rapidly to the highest
169 level and $\Delta\text{CO}/\Delta\text{CO}_2$ ratios were lower (MCE was higher) compared with the smoldering-dominated period. The fire
170 temperatures were very high during this initially high-efficiency burning period. During the later period, smoldering
171 dominated the burning conditions. The burning efficiency and fire temperatures decreased during this period, and
172 $\Delta\text{CO}/\Delta\text{CO}_2$ ratios were higher than the first period. Previous ground-based and aircraft measurements of wildfire emissions
173 also observed gradually decreased combustion efficiency of a fire over time (Collier et al., 2016). For the high-moisture



174 biomass burning, smoldering combustion dominated the fire types during the whole period (Figure 1b). Dehydration of the
175 higher moistures from biofuels consumed more heat released from the combustion, thus the burning efficiency and fire
176 temperatures were lower than those of the low-moisture biomass burning.

177 3.2 Emission factors of carbonaceous aerosols

178 The average emission factors of $PM_{2.5}$, OC and EC were 9.3 ± 3.4 , 4.6 ± 1.9 and 0.21 ± 0.07 g/kg for corn burning and
179 8.7 ± 5.0 , 3.9 ± 2.8 and 0.22 ± 0.05 g/kg for wheat burning (Figure 2). The particle EFs of corn burning were higher than wheat
180 burning, which is likely due to their different biomass structures, resulting in different pyrolysis temperatures and efficiency
181 (Zanatta et al., 2016). The measured emission factors in this study fall within the range of previous straw burning
182 experiments ($4.7\text{--}12.9$, $1.2\text{--}8.9$, $0.17\text{--}1.2$ g/kg for $PM_{2.5}$, OC and EC, respectively)(Akagi et al., 2011; Hays et al., 2005; Li et
183 al., 2007). The estimated EFs from crop residue burning were generally lower than wood or forest burning emissions (Akagi
184 et al., 2011; Aurell and Gullett, 2013; Jen et al., 2019). However, open crop residue burning in the field could result in severe
185 air pollution during harvest season, especially in agriculture areas in China and South Asia (IARI, 2012; Li et al., 2014;
186 Streets et al., 2003b; Venkataraman et al., 2006). This type of biomass burning cannot be negligible in these regions.

187 Organic matter (OM), calculated by multiplying OC by 1.3 (Li et al., 2007), was the dominant component of straw
188 burning aerosols, which accounted for ~64% and ~55% of the $PM_{2.5}$ emitted from corn and wheat burning (Figure 2).
189 Around 57% and 68% of the OC from corn and wheat burning are water soluble, and $HULIS_C$ represent 53% and 46% of the
190 WSOC. Though the mass contributions of WISOC were lower than WSOC in straw burning aerosols (Figure 2), the WISOC
191 fractions cannot be negligible, especially for considering the light absorption properties of BBOA (see section 3.4). Previous
192 studies also suggested a large portion of WISOC in ambient aerosols, which are important contributor of light-absorbing BrC
193 (Cheng et al., 2016; Cheng et al., 2017).

194 The average EFs of water-soluble acetic acid, formic acid, succinic acid and oxalic acid were respectively 13.3 ± 13.9 ,
195 4.1 ± 3.3 , 8.8 ± 0.6 , 2.2 ± 1.1 mg/kg for corn burning and 13.0 ± 14.5 , 4.7 ± 5.3 , 9.9 ± 13.5 , 3.1 ± 1.9 mg/kg for wheat burning
196 (Figure 2). Propionic acid and methanesulfonic acid in most samples were below the instrument detection limits in this study,
197 and their emissions were not taken into consideration in the following discussion. The quantified water-soluble
198 low-molecular-weight acids averagely accounted for 0.84% (0.16%–1.6%) and 0.88% (0.24%–1.8%) of the water-soluble
199 OM (WSOM) emitted from corn and wheat burning. Previous study has suggested that low molecular weight organic acids
200 represented an important fraction of WSOC in BBOA, and oxalic acid was a dominated short dicarboxylic (C2–C6) acids
201 (Falkovich et al., 2005). The estimated emission factors of acetic acid and formic acid in this work were lower than those
202 emitted from eucalypt forest fires, which were reported 17 and 26 mg/kg for flaming combustion, and 104 and 94 mg/kg for
203 smoldering combustion based on ground-based field measurements (Reisen et al., 2018). The difference could be attributed



204 to different biofuels, burning conditions as well as conducted experimental methods.

205 Figure 2 compares the emission factors of $PM_{2.5}$, carbonaceous aerosols and low molecular weight organic acids from
206 straw residue burning under different levels of moisture contents. The EFs of fine particles and organic carbonaceous
207 aerosols from high-moisture biomass burning were obviously higher than those from low-moisture biomass burning.
208 Substantial particulate carbonaceous aerosols could be generated from burning of higher-moisture biofuels, which is mainly
209 associated with the prolonged smoldering phases and less efficient combustions (Figure 1, Table S1). Similar variation trends
210 were also reported in previous biomass burning studies (Chen et al., 2010; Sanchis et al., 2014). Different levels of biofuel
211 moisture contents will actually influence the burning conditions, and thus impact the emission levels and compositions of
212 particulate matters.

213 3.3 Influence of combustion efficiency on emission factors

214 As shown in Figure 3, the emission factors of $PM_{2.5}$ and organic carbonaceous components increased with decreasing
215 MCE. Particle emissions were obviously enhanced under less efficient burning conditions. The emission factors of $PM_{2.5}$,
216 OC, WSOC and $HULIS_C$ from the most smoldering combustion experiment were about 3.4, 4.3, 3.8 and 2.8 times of those
217 from the most flaming combustion condition, regardless of the biomass types. The emissions of low molecular weight
218 organic acids also follow the similar variation trends with combustion efficiency as those of OC or WSOC emission factors
219 (Figure S2). These trends are generally in agreement with previous studies (Dhammapala et al., 2006; Holder et al., 2016;
220 Jen et al., 2019; Reisen et al., 2018; Wang et al., 2013). Under the same burning conditions, the emission factors of particles
221 or organic aerosols from corn burning were slightly higher than those from wheat burning (Figure 3). This was mainly due to
222 the different pyrolysis temperatures and combustion efficiency of different biofuels, which would influence the burning
223 processes (Khan et al., 2009; Zanatta et al., 2016). Our results suggested that the influence of varied burning conditions or
224 combustion efficiency on particle emissions could surpass the differences between the two types of straw residue burning
225 measured in this study (Figure 3). Thus, the burning efficiency or conditions should be taken into consideration when
226 simulate or estimate the influence of biomass burning emissions in future models.

227 Different from organic compounds, the emission factors of EC under different combustion efficiency remain relatively
228 consistent (Figure 3e). Holder et al. (2016) summarized the results from lab and field studies, and also found that the black
229 carbon emission factors from different studies are relatively constant, despite the differences in plume dilution or
230 measurement methods (Holder et al., 2016). Some studies, however, reported an increasing trend in EC or BC emission
231 levels with the increasing of combustion efficiency in wildfires or forest burns in U.S. (Aurell and Gullett, 2013; Jen et al.,
232 2019). As the conducted experiments were mostly dominated by smoldering combustions (MCE=0.68-0.88) in this study, we
233 cannot exclude the possibility that the EC emissions may be higher under flaming-dominated combustions (e.g. MCE>0.9).



234 Though the less variations of EC emission factors as a function of MCE, a positive correlation between EC/(OC+EC) ratios
235 and combustion efficiency was observed (Figure 3g). Due to the obvious dependence of EC/OC or EC/(OC+EC) ratios on
236 burning efficiency, these ratios could be employed to indicate different burning conditions when the emitted CO and CO₂
237 data is not available, which have been used in previous studies (Xie et al., 2018; Xie et al., 2019).

238 To further investigate the influence of burning conditions on the chemical compositions of biomass burning aerosols,
239 mass ratios of WSOC/OC, HULIS_C/OC, K⁺/OC and Cl⁻/OC as a function of burning efficiency are plotted in Figure 4. The
240 WSOC/OC and HULIS_C/OC mass ratios ranged from 0.52-0.78 and 0.16-0.54 among different burning experiments. The
241 HULIS_C/OC ratios were comparable to those (0.26-0.44, with an average of 0.34) reported in field or controlled chamber
242 combustion experiments (Lin et al., 2010). We did not observe obvious variation trends of WSOC/OC or HULIS_C/OC ratios
243 with MCE (Figure 4), which indicated relative constant BBOA chemical compositions under different combustion conditions.
244 However, the K⁺/OC and Cl⁻/OC ratios showed consistent variation trends under different MCE conditions, which increased
245 from <0.1 under the more smoldering condition to >0.5 under the more flaming condition for K⁺/OC, and from 0.05 to >0.5
246 for Cl⁻/OC (Figure 4). The highest K⁺/OC (0.64) and Cl⁻/OC (0.61) ratios were observed in a low-moisture wheat burning
247 experiment with a MCE of 0.79. This is because that the K and Cl emissions from combustion are highly affected by fire
248 temperatures and burning conditions. Lab-controlled experiments suggested that the proportions of released potassium and
249 chlorine from the biomass fuels increase with the applied combustion temperatures (Jensen et al., 2000; Knudsen et al.,
250 2004). The flaming combustion (with higher MCE) was observed much higher fire temperatures than the smoldering
251 combustion (with lower MCE) (Figure 1). Though the emission levels of particles or organic aerosols decreased during
252 higher efficiency burning (Figure 3), elevated proportions of potassium and chlorine were released into smokes during the
253 flaming combustion phase under this condition (Figure 4b). Potassium ion is a commonly used tracer to indicate the biomass
254 burning emissions. However, our results revealed that K⁺ cannot correctly indicate the emission levels of biomass burning
255 aerosols under obviously different burning conditions, which may lead to large uncertainty in estimating burning emissions if
256 without considering the combustion conditions.

257 3.4 Light absorption of BBOA

258 The light absorption of straw burning organic aerosols decreased sharply from near-UV to visible wavelengths (Figure
259 5), indicating their properties as biomass burning-generated BrC. The absorption of WISOC, WSOC and HULIS_C at 300 nm
260 was as high as 4.5, 15.2 and 11.2 times of those at 400 nm for corn burning emissions, and 4.8, 9.2 and 10.6 times for wheat
261 burning emissions. The wavelength dependence property of BBOA light absorption was described by AAE derived from the
262 absorption in the range of 300-450 nm. The AAE of WISOC, WSOC and HULIS_C were respectively 5.8-5.9, 8.6-11.3,
263 8.9-10.2 for corn burning aerosols and 5.7-6.0, 8.1-9.0, 9.0-10.5 for wheat burning aerosols, and the averaged values were



264 also shown in Figure 5. The water-soluble BBOA fractions (WSOC and HULIS) showed stronger wavelength dependence
265 than the water insoluble fractions. The estimated AAE values of straw burning organic aerosols in this study are comparable
266 to those of BBOA (5.3-8.1) and biomass burning-influenced atmospheric aerosols (5.2-9.4) reported in previous studies
267 (Hecobian et al., 2010; Hoffer et al., 2006; Wu et al., 2018; Wu et al., 2019; Xie et al., 2017; Xie et al., 2019; Zhu et al.,
268 2018). The strong light absorption of biomass burning-generated BrC in near-UV range would lead to an increase in aerosol
269 light absorption and radiative forcing efficiency (Chakrabarty et al., 2010).

270 The WISOC was the most important light-absorption fraction among straw burning organic aerosols, which contributed
271 61%–84% and 57%–72% of the light absorption (@300-400 nm) by extracted BrC emitted from corn and wheat burning
272 (Figure 5). HULIS_C and other high-polarity WSOC (WSOC-h=WSOC-HULIS_C) respectively occupy 16%-28% and 1%-10%
273 of the BBOA absorption at 300-400 nm for corn burning, and 17%-29% and 12%-15% for wheat burning. Though the mass
274 contribution of WISOC was lower than WSOC (Figure 2), the light absorption of WISOC surpassed WSOC due to the
275 higher light absorption capability of water-insoluble BBOA, indicated by the higher MAE of WISOC (Figure 6). Meanwhile,
276 the light absorption of water-soluble BBOA among near-UV ranges cannot be neglected due to their sharper increase of
277 absorption towards shorter wavelength compared with WISOC (Figure 5). The light absorption contribution of WSOC to
278 extracted BrC increased substantially from 16%-28% at 400 nm to 39%-43% at 300 nm. Among the water-soluble BBOA,
279 HULIS were the major contributors of light absorption, which occupied 74% and 68% of the WSOC absorption at 300 nm
280 for corn and wheat burning emissions, respectively. This was due to the higher light absorption capability of HULIS than
281 other high-polarity WSOC fractions (Figure 6), though their mass contributions were comparable in straw burning aerosols
282 (Figure 2).

283 The light absorption capabilities of different BBOA fractions are compared in Figure 6. The estimated MAE₃₆₅ values of
284 straw burning-generated BrC in this study are comparable to those reported in previous studies (Fan et al., 2018; Xie et al.,
285 2017). The MAE of WISOC are higher than water-soluble BBOA (WSOC and HULIS) among the measured wavelength
286 ranges for both corn and wheat burning aerosols. The MAE₃₀₀ of WISOC was 1.6 and 1.7 times of WSOC emitted from corn
287 and wheat burning, and comparable to those of HULIS (Figure 6). Due to the slower decrease of WISOC absorption towards
288 visible wavelengths than the water-soluble fractions (Figure 5), the MAE₃₆₅ of WISOC was as high as 2.5 and 2.2 times of
289 WSOC from corn and wheat burning emissions, and 1.7 and 1.6 times of HULIS. Though the mass contribution of WISOC
290 among BBOA could be smaller than WSOC, their contribution to light absorption cannot be neglected due to the higher
291 MAE of water insoluble BBOA. The light absorption of BBOA would be largely underestimated if only considering the
292 water soluble fractions. Previous studies also reported a large proportion of WISOC absorption in BBOA and ambient
293 aerosols (Cheng et al., 2016; Cheng et al., 2017; Park et al., 2018; Sengupta et al., 2018).



294 Figure 7 clearly shows the dependence of BBOA absorption coefficient (Abs_{365}) on burning conditions. Higher Abs_{365}
295 of biomass burning-generated BrC were observed under less efficient burning conditions for both corn and wheat burning
296 experiments. This is mainly due to the elevated BBOA emission factors as the decreasing of MCE (Figure 3). Furthermore,
297 the MAE_{365} of WSOC and HULIS emitted from straw burning were slightly higher under less efficient burning conditions
298 (Figures 7d, 7e). For the WISOC, however, we did not observe obvious dependence of MAE_{365} on the combustion efficiency
299 (Figure 7f). Previous lab and field studies suggested that the optical properties of biomass burning aerosols are more
300 dependent on burning conditions other than fuel types (Liu et al., 2014; Xie et al., 2017). The MAE_{365} of BBOA emitted
301 from flaming combustion were reported higher than those from smoldering combustion based on lab-controlled burning
302 experiments (Xie et al., 2019). Another lab experiment also suggested the dependence of MAE_{365} of methanol-extracted
303 BBOA on burning conditions, while the variation trends are different regarding different fuel types or sampling methods
304 among different experiments (Xie et al., 2017). It is noted that limited sample population was selected to conduct the light
305 absorption measurements in this study, and we did not observe a significant correlation between MAE and combustion
306 conditions. More lab experiments are required to address the influence of combustion efficiency on light absorption
307 capability of biomass burning-emitted carbonaceous aerosols.

308 4 Conclusions

309 The emission factors of $PM_{2.5}$, OC and EC were 9.3, 4.6 and 0.21 g/kg for corn burning and 8.7, 3.9 and 0.22 g/kg for
310 wheat burning, generally lower than wood or forest burning emissions. Around 57% and 68% of the OC emitted from corn
311 and wheat burning are WSOC, among which $HULIS_C$ represent 53% and 46% of the WSOC mass concentrations. Though
312 the mass contribution of WISOC was lower than WSOC, the light absorption contribution of WISOC (57%–84% @300-400
313 nm) surpassed WSOC due to the higher MAE of WISOC. The BBOA light absorption would be largely underestimated if
314 only considering the water soluble fractions. Meanwhile, the light absorption of WSOC among near-UV ranges, occupying
315 39%–43% of extracted OC absorption at 300 nm, cannot be negligible due to their sharper increase of absorption towards
316 shorter wavelength compared with WISOC. HULIS were the major light absorption contributors among WSOC, and their
317 light absorption capability was higher than other high-polarity WSOC components.

318 The emission levels, compositions and light absorption of BBOA were largely influenced by the burning conditions and
319 biofuel moisture contents. The combustion conditions varied from different burning experiments, with the MCE ranging
320 from 0.68 to 0.88. The emission factors of $PM_{2.5}$ and organic carbonaceous aerosols were obviously enhanced under less
321 efficient burning conditions (lower MCE). The emission factors of $PM_{2.5}$, OC, WSOC and $HULIS_C$ from the most
322 smoldering combustion experiment were about 3.4, 4.3, 3.8 and 2.8 times of those from the most flaming combustion
323 condition, regardless of the biofuel types employed in this study. The emission factors of $PM_{2.5}$ and carbonaceous aerosols



324 from high-moisture straw burning were obviously elevated compared with those from low-moisture straw burning
325 experiments. This is mainly due to the prolonged smoldering and incomplete combustion period during high-moisture
326 biomass burning.

327 The EC/(EC+OC) ratios showed a positive correlation with MCE, though EC emission factors remain relative constant
328 under different combustion conditions. Thus, it is reasonable to employ EC/OC or EC/(EC+OC) ratios as an indicator of
329 biomass burning conditions. The mass ratios of WSOC/OC or HULIS_c/OC did not display obvious variation trends under
330 different combustion efficiency. However, the K⁺/OC and Cl⁻/OC ratios showed continuous increasing trends during higher
331 efficiency burning, from <0.1 under the more smoldering condition to >0.5 under the more flaming condition for K⁺/OC, and
332 from 0.05 to >0.5 for Cl⁻/OC ratios. This is mainly attributed to the elevated proportions of released potassium and chlorine
333 from biofuels under the higher fire temperatures during flaming combustions. Our results indicate that potassium ion, as a
334 commonly used biomass burning tracer, may lead to large uncertainty in estimating biomass burning emission levels if
335 without considering the combustion conditions.

336 Higher absorption coefficient (Abs₃₆₅) of straw burning-generated BrC, including WSOC, HULIS and WISOC, were
337 observed under less efficient burning conditions for both corn and wheat burning. This is mainly attributed to the higher
338 BBOA emission factors as the decreasing of MCE. In addition, the MAE₃₆₅ of WSOC and HULIS emitted from straw
339 burning were slightly higher under low-MCE conditions. Our results suggested that the influence of varied combustion
340 efficiency on the emission levels and light absorption of BBOA could surpass the differences between biofuel types. Thus,
341 the burning efficiency or combustion conditions should be taken into consideration when estimate the influence of biomass
342 burning.

343

344

345 *Data availability.* The data presented in this article are available from the authors upon request (minhu@pku.edu.cn).

346

347 The Supplement related to this article is available online

348

349 *Author contributions.* MH, ZW, XH, and LH organized the project. YW conducted the simulation experiments. YW, NX and
350 YQ analyzed the samples. YW wrote the manuscript with input from all co-authors. All authors contributed to discussing the
351 results and commenting on the manuscript.

352

353 *Competing interests.* The authors declare that they have no conflict of interest.

354



355 *Acknowledgements.* This work was supported by National Natural Science Foundation of China (91844301, 91544214), and
356 the project funded by China Postdoctoral Science Foundation (2019M650354). We also thank Dr. Song Guo for his helpful
357 suggestions on this work.

358

359

360 **References:**

- 361 Crop Residues Management with Conservation Agriculture: Potential, Constraints and Policy Needs, edited by: Institute, I. A.
362 R., India, 2012.
- 363 Akagi, S. K., Yokelson, R. J., Wiedinmyer, C., Alvarado, M. J., Reid, J. S., Karl, T., Crouse, J. D., and Wennberg, P. O.:
364 Emission factors for open and domestic biomass burning for use in atmospheric models, *Atmos. Chem. Phys.*, 11, 4039-4072,
365 10.5194/acp-11-4039-2011, 2011.
- 366 Andreae, M. O. and Merlet, P.: Emission of trace gases and aerosols from biomass burning, *Global Biogeochem. Cy.*, 15,
367 955-966, Doi 10.1029/2000gb001382, 2001.
- 368 Andreae, M. O. and Gelencsík, A.: Black carbon or brown carbon? The nature of light-absorbing carbonaceous aerosols,
369 *Atmos. Chem. Phys.*, 6, 3131-3148, 10.5194/acp-6-3131-2006, 2006.
- 370 Aurell, J. and Gullett, B. K.: Emission factors from aerial and ground measurements of field and laboratory forest burns in
371 the southeastern US: PM_{2.5}, black and brown carbon, VOC, and PCDD/PCDF, *Environ. Sci. Technol.*, 47, 8443-8452,
372 10.1021/es402101k, 2013.
- 373 Bond, T. C.: A technology-based global inventory of black and organic carbon emissions from combustion, *J. Geophys. Res.*,
374 109, 10.1029/2003jd003697, 2004.
- 375 Bond, T. C., Doherty, S. J., Fahey, D. W., Forster, P. M., Berntsen, T., DeAngelo, B. J., Flanner, M. G., Ghan, S., Köhler, B.,
376 Koch, D., Kinne, S., Kondo, Y., Quinn, P. K., Sarofim, M. C., Schultz, M. G., Schulz, M., Venkataraman, C., Zhang, H.,
377 Zhang, S., Bellouin, N., Guttikunda, S. K., Hopke, P. K., Jacobson, M. Z., Kaiser, J. W., Klimont, Z., Lohmann, U., Schwarz,
378 J. P., Shindell, D., Storelvmo, T., Warren, S. G., and Zender, C. S.: Bounding the role of black carbon in the climate system:
379 A scientific assessment, *J. Geophys. Res.*, [Atmos.], 118, 5380-5552, 10.1002/jgrd.50171, 2013.
- 380 Chakrabarty, R. K., Moosmüller, H., Chen, L. W. A., Lewis, K., Arnott, W. P., Mazzoleni, C., Dubey, M. K., Wold, C. E.,
381 Hao, W. M., and Kreidenweis, S. M.: Brown carbon in tar balls from smoldering biomass combustion, *Atmos. Chem. Phys.*,
382 10, 6363-6370, 10.5194/acp-10-6363-2010, 2010.
- 383 Chen, J., Li, C., Ristovski, Z., Milic, A., Gu, Y., Islam, M. S., Wang, S., Hao, J., Zhang, H., He, C., Guo, H., Fu, H., Miljevic,
384 B., Morawska, L., Thai, P., Lam, Y. F., Pereira, G., Ding, A., Huang, X., and Dumka, U. C.: A review of biomass burning:
385 Emissions and impacts on air quality, health and climate in China, *Sci. Total Environ.*, 579, 1000-1034,
386 10.1016/j.scitotenv.2016.11.025, 2017a.
- 387 Chen, L. W. A., Verburg, P., Shackelford, A., Zhu, D., Susfalk, R., Chow, J. C., and Watson, J. G.: Moisture effects on carbon
388 and nitrogen emission from burning of wildland biomass, *Atmos. Chem. Phys.*, 10, 6617-6625, 10.5194/acp-10-6617-2010,
389 2010.
- 390 Chen, Q., Ikemori, F., Higo, H., Asakawa, D., and Mochida, M.: Chemical Structural Characteristics of HULIS and Other
391 Fractionated Organic Matter in Urban Aerosols: Results from Mass Spectral and FT-IR Analysis, *Environ. Sci. Technol.*, 50,
392 1721-1730, 10.1021/acs.est.5b05277, 2016a.
- 393 Chen, Q., Ikemori, F., and Mochida, M.: Light Absorption and Excitation-Emission Fluorescence of Urban Organic Aerosol
394 Components and Their Relationship to Chemical Structure, *Environ. Sci. Technol.*, 50, 10859-10868,
395 10.1021/acs.est.6b02541, 2016b.
- 396 Chen, Q., Ikemori, F., Nakamura, Y., Vodicka, P., Kawamura, K., and Mochida, M.: Structural and Light-Absorption
397 Characteristics of Complex Water-Insoluble Organic Mixtures in Urban Submicrometer Aerosols, *Environ. Sci. Technol.*, 51,
398 8293-8303, 10.1021/acs.est.7b01630, 2017b.



- 399 Chen, Y. and Bond, T. C.: Light absorption by organic carbon from wood combustion, *Atmos. Chem. Phys.*, 10, 1773-1787,
400 10.5194/acp-10-1773-2010, 2010.
- 401 Cheng, Y., He, K. B., Zheng, M., Duan, F. K., Du, Z. Y., Ma, Y. L., Tan, J. H., Yang, F. M., Liu, J. M., Zhang, X. L., Weber, R.
402 J., Bergin, M. H., and Russell, A. G.: Mass absorption efficiency of elemental carbon and water-soluble organic carbon in
403 Beijing, China, *Atmos. Chem. Phys.*, 11, 11497-11510, 10.5194/acp-11-11497-2011, 2011.
- 404 Cheng, Y., Engling, G., He, K. B., Duan, F. K., Ma, Y. L., Du, Z. Y., Liu, J. M., Zheng, M., and Weber, R. J.: Biomass
405 burning contribution to Beijing aerosol, *Atmos. Chem. Phys.*, 13, 7765-7781, 10.5194/acp-13-7765-2013, 2013.
- 406 Cheng, Y., He, K.-b., Du, Z.-y., Engling, G., Liu, J.-m., Ma, Y.-l., Zheng, M., and Weber, R. J.: The characteristics of brown
407 carbon aerosol during winter in Beijing, *Atmos. Environ.*, 127, 355-364, 10.1016/j.atmosenv.2015.12.035, 2016.
- 408 Cheng, Y., He, K. B., Engling, G., Weber, R., Liu, J. M., Du, Z. Y., and Dong, S. P.: Brown and black carbon in Beijing
409 aerosol: Implications for the effects of brown coating on light absorption by black carbon, *Sci. Total Environ.*, 599-600,
410 1047-1055, 10.1016/j.scitotenv.2017.05.061, 2017.
- 411 Collier, S., Zhou, S., Onasch, T. B., Jaffe, D. A., Kleinman, L., Sedlacek, A. J., 3rd, Briggs, N. L., Hee, J., Fortner, E.,
412 Shilling, J. E., Worsnop, D., Yokelson, R. J., Parworth, C., Ge, X., Xu, J., Butterfield, Z., Chand, D., Dubey, M. K., Pekour,
413 M. S., Springston, S., and Zhang, Q.: Regional Influence of Aerosol Emissions from Wildfires Driven by Combustion
414 Efficiency: Insights from the BBOP Campaign, *Environ. Sci. Technol.*, 50, 8613-8622, 10.1021/acs.est.6b01617, 2016.
- 415 Dhammapala, R., Claiborn, C., Corkill, J., and Gullett, B.: Particulate emissions from wheat and Kentucky bluegrass stubble
416 burning in eastern Washington and northern Idaho, *Atmos. Environ.*, 40, 1007-1015, 10.1016/j.atmosenv.2005.11.018, 2006.
- 417 Falkovich, A. H., Graber, E. R., Schkolnik, G., Rudich, Y., Maenhaut, W., and Artaxo, P.: Low molecular weight organic
418 acids in aerosol particles from Rondônia, Brazil, during the biomass-burning, transition and wet periods, *Atmos. Chem.
419 Phys.*, 5, 781-797, 10.5194/acp-5-781-2005, 2005.
- 420 Fan, X., Li, M., Cao, T., Cheng, C., Li, F., Xie, Y., Wei, S., Song, J., and Peng, P. a.: Optical properties and oxidative
421 potential of water- and alkaline-soluble brown carbon in smoke particles emitted from laboratory simulated biomass burning,
422 *Atmos. Environ.*, 194, 48-57, 10.1016/j.atmosenv.2018.09.025, 2018.
- 423 Feng, Y., Ramanathan, V., and Kotamarthi, V. R.: Brown carbon: a significant atmospheric absorber of solar radiation?,
424 *Atmos. Chem. Phys.*, 13, 8607-8621, 10.5194/acp-13-8607-2013, 2013.
- 425 Guo, S., Hu, M., Wang, Z. B., Slanina, J., and Zhao, Y. L.: Size-resolved aerosol water-soluble ionic compositions in the
426 summer of Beijing: implication of regional secondary formation, *Atmos. Chem. Phys.*, 10, 947-959,
427 10.5194/acp-10-947-2010, 2010.
- 428 Hays, M. D., Fine, P. M., Geron, C. D., Kleeman, M. J., and Gullett, B. K.: Open burning of agricultural biomass: Physical
429 and chemical properties of particle-phase emissions, *Atmos. Environ.*, 39, 6747-6764, 10.1016/j.atmosenv.2005.07.072,
430 2005.
- 431 He, L. Y., Lin, Y., Huang, X. F., Guo, S., Xue, L., Su, Q., Hu, M., Luan, S. J., and Zhang, Y. H.: Characterization of
432 high-resolution aerosol mass spectra of primary organic aerosol emissions from Chinese cooking and biomass burning,
433 *Atmos. Chem. Phys.*, 10, 11535-11543, 10.5194/acp-10-11535-2010, 2010.
- 434 Hecobian, A., Zhang, X., Zheng, M., Frank, N., Edgerton, E. S., and Weber, R. J.: Water-Soluble Organic Aerosol material
435 and the light-absorption characteristics of aqueous extracts measured over the Southeastern United States, *Atmos. Chem.
436 Phys.*, 10, 5965-5977, 10.5194/acp-10-5965-2010, 2010.
- 437 Hoffer, A., Gelencsér, A., Guyon, P., Kiss, G., Schmid, O., Frank, G. P., Artaxo, P., and Andreae, M. O.: Optical properties of
438 humic-like substances (HULIS) in biomass-burning aerosols, *Atmos. Chem. Phys.*, 6, 3563-3570, 10.5194/acp-6-3563-2006,
439 2006.
- 440 Holder, A. L., Hagler, G. S. W., Aurell, J., Hays, M. D., and Gullett, B. K.: Particulate matter and black carbon optical
441 properties and emission factors from prescribed fires in the southeastern United States, *J. Geophys. Res.*, [Atmos.], 121,
442 3465-3483, 10.1002/2015jd024321, 2016.
- 443 Hungershofer, K., Zeromskiene, K., Iinuma, Y., Helas, G., Trentmann, J., Trautmann, T., Parmar, R. S., Wiedensohler, A.,
444 Andreae, M. O., and Schmid, O.: Modelling the optical properties of fresh biomass burning aerosol produced in a smoke
445 chamber: results from the EFEU campaign, *Atmos. Chem. Phys.*, 8, 3427-3439, 10.5194/acp-8-3427-2008, 2008.



- 446 Jen, C. N., Hatch, L. E., Selimovic, V., Yokelson, R. J., Weber, R., Fernandez, A. E., Kreisberg, N. M., Barsanti, K. C., and
447 Goldstein, A. H.: Speciated and total emission factors of particulate organics from burning western US wildland fuels and
448 their dependence on combustion efficiency, *Atmos. Chem. Phys.*, 19, 1013-1026, 10.5194/acp-19-1013-2019, 2019.
- 449 Jensen, P. A., Frandsen, F. J., Dam-Johansen, K., and Sander, B.: Experimental Investigation of the Transformation and
450 Release to Gas Phase of Potassium and Chlorine during Straw Pyrolysis, *Energ Fuel*, 14, 1280-1285, 10.1021/ef000104v,
451 2000.
- 452 Khan, A. A., de Jong, W., Jansens, P. J., and Spliethoff, H.: Biomass combustion in fluidized bed boilers: Potential problems
453 and remedies, *Fuel Processing Technology*, 90, 21-50, 10.1016/j.fuproc.2008.07.012, 2009.
- 454 Knudsen, J. N., Jensen, P. A., and Dam-Johansen, K.: Transformation and release to the gas phase of Cl, K, and S during
455 combustion of annual biomass, *Energ Fuel*, 18, 1385-1399, 10.1021/ef049944q, 2004.
- 456 Laskin, A., Laskin, J., and Nizkorodov, S. A.: Chemistry of atmospheric brown carbon, *Chem. Rev.*, 115, 4335-4382,
457 10.1021/cr5006167, 2015.
- 458 Li, J. F., Song, Y., Mao, Y., Mao, Z. C., Wu, Y. S., Li, M. M., Huang, X., He, Q. C., and Hu, M.: Chemical characteristics and
459 source apportionment of PM_{2.5} during the harvest season in eastern China's agricultural regions, *Atmos. Environ.*, 92,
460 442-448, 10.1016/j.atmosenv.2014.04.058, 2014.
- 461 Li, M., Fan, X., Zhu, M., Zou, C., Song, J., Wei, S., Jia, W., and Peng, P.: Abundances and light absorption properties of
462 brown carbon emitted from residential coal combustion in China, *Environ. Sci. Technol.*, 53, 595-603,
463 10.1021/acs.est.8b05630, 2018.
- 464 Li, X., Wang, S., Duan, L., Hao, J., Li, C., Chen, Y., and Yang, L.: Particulate and trace gas emissions from open burning of
465 wheat straw and corn stover in China, *Environ. Sci. Technol.*, 41, 6052-6058, 10.1021/es0705137, 2007.
- 466 Lin, P., Engling, G., and Yu, J. Z.: Humic-like substances in fresh emissions of rice straw burning and in ambient aerosols in
467 the Pearl River Delta Region, China, *Atmos. Chem. Phys.*, 10, 6487-6500, 10.5194/acp-10-6487-2010, 2010.
- 468 Lin, P. and Yu, J. Z.: Generation of reactive oxygen species mediated by humic-like substances in atmospheric aerosols,
469 *Environ. Sci. Technol.*, 45, 10362-10368, 10.1021/es2028229, 2011.
- 470 Lin, P., Aiona, P. K., Li, Y., Shiraiwa, M., Laskin, J., Nizkorodov, S. A., and Laskin, A.: Molecular characterization of brown
471 carbon in biomass burning aerosol particles, *Environ. Sci. Technol.*, 50, 11815-11824, 10.1021/acs.est.6b03024, 2016.
- 472 Liu, J., Bergin, M., Guo, H., King, L., Kotra, N., Edgerton, E., and Weber, R. J.: Size-resolved measurements of brown
473 carbon in water and methanol extracts and estimates of their contribution to ambient fine-particle light absorption, *Atmos.*
474 *Chem. Phys.*, 13, 12389-12404, 10.5194/acp-13-12389-2013, 2013.
- 475 Liu, S., Aiken, A. C., Arata, C., Dubey, M. K., Stockwell, C. E., Yokelson, R. J., Stone, E. A., Jayarathne, T., Robinson, A. L.,
476 DeMott, P. J., and Kreidenweis, S. M.: Aerosol single scattering albedo dependence on biomass combustion efficiency:
477 Laboratory and field studies, *Geophys. Res. Lett.*, 41, 742-748, 10.1002/2013gl058392, 2014.
- 478 Park, S., Yu, G.-H., and Lee, S.: Optical absorption characteristics of brown carbon aerosols during the KORUS-AQ
479 campaign at an urban site, *Atmos. Res.*, 203, 16-27, 10.1016/j.atmosres.2017.12.002, 2018.
- 480 Reid, J. S., Eck, T. F., Christopher, S. A., Koppmann, R., Dubovik, O., Eleuterio, D. P., Holben, B. N., Reid, E. A., and
481 Zhang, J.: A review of biomass burning emissions part III: intensive optical properties of biomass burning particles, *Atmos.*
482 *Chem. Phys.*, 5, 827-849, 10.5194/acp-5-827-2005, 2005.
- 483 Reisen, F., Meyer, C. P., Weston, C. J., and Volkova, L.: Ground-Based Field Measurements of PM_{2.5} Emission Factors From
484 Flaming and Smoldering Combustion in Eucalypt Forests, *J. Geophys. Res.*, [Atmos.], 10.1029/2018jd028488, 2018.
- 485 Saleh, R., Robinson, E. S., Tkacik, D. S., Ahern, A. T., Liu, S., Aiken, A. C., Sullivan, R. C., Presto, A. A., Dubey, M. K.,
486 Yokelson, R. J., Donahue, N. M., and Robinson, A. L.: Brownness of organics in aerosols from biomass burning linked to
487 their black carbon content, *Nature Geosci.*, 7, 647-650, 10.1038/ngeo2220, 2014.
- 488 Saleh, R., Marks, M., Heo, J., Adams, P. J., Donahue, N. M., and Robinson, A. L.: Contribution of brown carbon and lensing
489 to the direct radiative effect of carbonaceous aerosols from biomass and biofuel burning emissions, *J. Geophys. Res.*,
490 [Atmos.], 120, 10.1002/2015jd023697, 2015.
- 491 Sanchis, E., Ferrer, M., Calvet, S., Coscollà C., Yúsà V., and Cambra-López, M.: Gaseous and particulate emission profiles
492 during controlled rice straw burning, *Atmos. Environ.*, 98, 25-31, 10.1016/j.atmosenv.2014.07.062, 2014.



493 Sengupta, D., Samburova, V., Bhattarai, C., Kirillova, E., Mazzoleni, L., Iaukea-Lum, M., Watts, A., Moosmüller, H., and
494 Khlystov, A.: Light absorption by polar and non-polar aerosol compounds from laboratory biomass combustion, *Atmos.*
495 *Chem. Phys.*, 18, 10849-10867, 10.5194/acp-18-10849-2018, 2018.

496 Streets, D. G., Yarber, K. F., Woo, J. H., and Carmichael, G. R.: Biomass burning in Asia: Annual and seasonal estimates and
497 atmospheric emissions, *Global Biogeochem. Cy.*, 17, n/a-n/a, 10.1029/2003gb002040, 2003a.

498 Streets, D. G., Yarber, K. F., Woo, J. H., and Carmichael, G. R.: Biomass burning in Asia: Annual and seasonal estimates and
499 atmospheric emissions, *Global Biogeochem. Cy.*, 17, Artn 1099 10.1029/2003gb002040, 2003b.

500 Venkataraman, C., Habib, G., Kadamba, D., Shrivastava, M., Leon, J. F., Crouzille, B., Boucher, O., and Streets, D. G.:
501 Emissions from open biomass burning in India: Integrating the inventory approach with high-resolution Moderate Resolution
502 Imaging Spectroradiometer (MODIS) active-fire and land cover data, *Global Biogeochem. Cy.*, 20, GB2013,
503 10.1029/2005gb002547, 2006.

504 Wang, Q., Itoh, S., Itoh, K., Apaer, P., Chen, Q., Niida, D., Mitsumura, N., Animesh, S., Sekiguchi, K., and Endo, T.:
505 Behavior of suspended particulate matter emitted from combustion of agricultural residue biomass under different
506 temperatures, 1, 3-13, 10.2495/esus130271, 2013.

507 Wang, Y., Hu, M., Lin, P., Guo, Q., Wu, Z., Li, M., Zeng, L., Song, Y., Zeng, L., Wu, Y., Guo, S., Huang, X., and He, L.:
508 Molecular characterization of nitrogen-containing organic compounds in humic-like substances emitted from straw residue
509 burning, *Environ. Sci. Technol.*, 51, 5951-5961, 10.1021/acs.est.7b00248, 2017.

510 Washenfelder, R. A., Attwood, A. R., Brock, C. A., Guo, H., Xu, L., Weber, R. J., Ng, N. L., Allen, H. M., Ayres, B. R.,
511 Baumann, K., Cohen, R. C., Draper, D. C., Duffey, K. C., Edgerton, E., Fry, J. L., Hu, W. W., Jimenez, J. L., Palm, B. B.,
512 Romer, P., Stone, E. A., Wooldridge, P. J., and Brown, S. S.: Biomass burning dominates brown carbon absorption in the
513 rural southeastern United States, *Geophys. Res. Lett.*, 42, 653-664, 10.1002/2014gl062444, 2015.

514 Wu, G., Wan, X., Gao, S., Fu, P., Yin, Y., Li, G., Zhang, G., Kang, S., Ram, K., and Cong, Z.: Humic-like substances (HULIS)
515 in aerosols of central Tibetan Plateau (Nam Co, 4730 m asl): Abundance, light absorption properties, and sources, *Environ.*
516 *Sci. Technol.*, 52, 7203-7211, 10.1021/acs.est.8b01251, 2018.

517 Wu, G., Ram, K., Fu, P., Wang, W., Zhang, Y., Liu, X., Stone, E. A., Pradhan, B. B., Dangol, P. M., Panday, A. K., Wan, X.,
518 Bai, Z., Kang, S., Zhang, Q., and Cong, Z.: Water-soluble brown carbon in atmospheric aerosols from Godavari (Nepal), a
519 regional representative of South Asia, *Environ. Sci. Technol.*, 53, 3471-3479, 10.1021/acs.est.9b00596, 2019.

520 Xie, M., Hays, M. D., and Holder, A. L.: Light-absorbing organic carbon from prescribed and laboratory biomass burning
521 and gasoline vehicle emissions, *Scientific reports*, 7, 7318, 10.1038/s41598-017-06981-8, 2017.

522 Xie, M., Shen, G., Holder, A. L., Hays, M. D., and Jetter, J. J.: Light absorption of organic carbon emitted from burning
523 wood, charcoal, and kerosene in household cookstoves, *Environ. Pollut.*, 240, 60-67, 10.1016/j.envpol.2018.04.085, 2018.

524 Xie, M., Chen, X., Hays, M. D., and Holder, A. L.: Composition and light absorption of N-containing aromatic compounds
525 in organic aerosols from laboratory biomass burning, *Atmos Chem Phys*, 19, 2899-2915, 10.5194/acp-19-2899-2019, 2019.

526 Yan, J., Wang, X., Gong, P., Wang, C., and Cong, Z.: Review of brown carbon aerosols: Recent progress and perspectives,
527 *Sci. Total Environ.*, 634, 1475-1485, 10.1016/j.scitotenv.2018.04.083, 2018.

528 Zanatta, E. R., Reinehr, T. O., Awadallak, J. A., Klein übing, S. J., dos Santos, J. B. O., Bariccatti, R. A., Arroyo, P. A., and da
529 Silva, E. A.: Kinetic studies of thermal decomposition of sugarcane bagasse and cassava bagasse, *J. Therm. Anal. Calorim.*,
530 125, 437-445, 10.1007/s10973-016-5378-x, 2016.

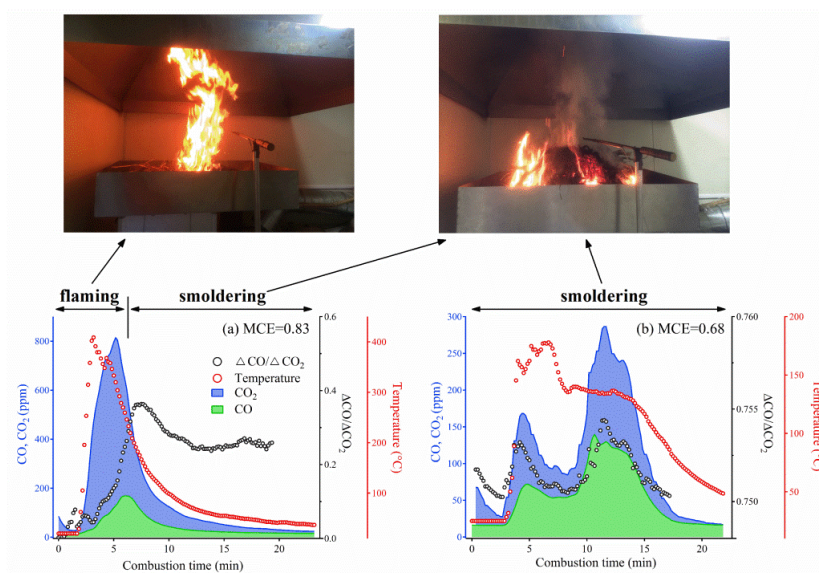
531 Zhang, G., Li, J., Li, X. D., Xu, Y., Guo, L. L., Tang, J. H., Lee, C. S., Liu, X., and Chen, Y. J.: Impact of anthropogenic
532 emissions and open biomass burning on regional carbonaceous aerosols in South China, *Environ. Pollut.*, 158, 3392-3400,
533 10.1016/j.envpol.2010.07.036, 2010.

534 Zhu, C. S., Cao, J. J., Huang, R. J., Shen, Z. X., Wang, Q. Y., and Zhang, N. N.: Light absorption properties of brown carbon
535 over the southeastern Tibetan Plateau, *Sci. Total Environ.*, 625, 246-251, 10.1016/j.scitotenv.2017.12.183, 2018.

536
537
538
539



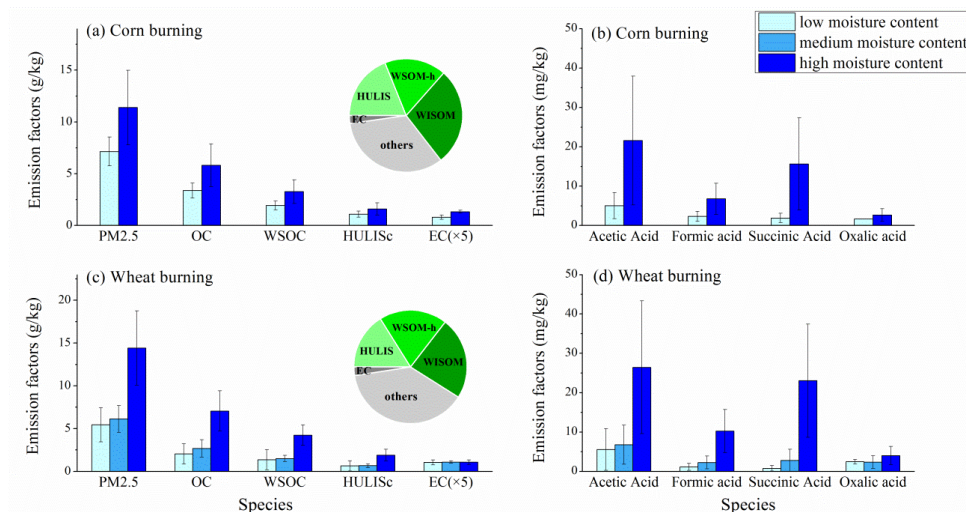
540 **Figures**



541

542 Figure 1 Variations of measured CO, CO₂ concentrations, $\Delta\text{CO}/\Delta\text{CO}_2$, fire temperatures and burning conditions during two
 543 selected experiments, with an averaged MCE value of (a) 0.83 and (b) 0.68.

544

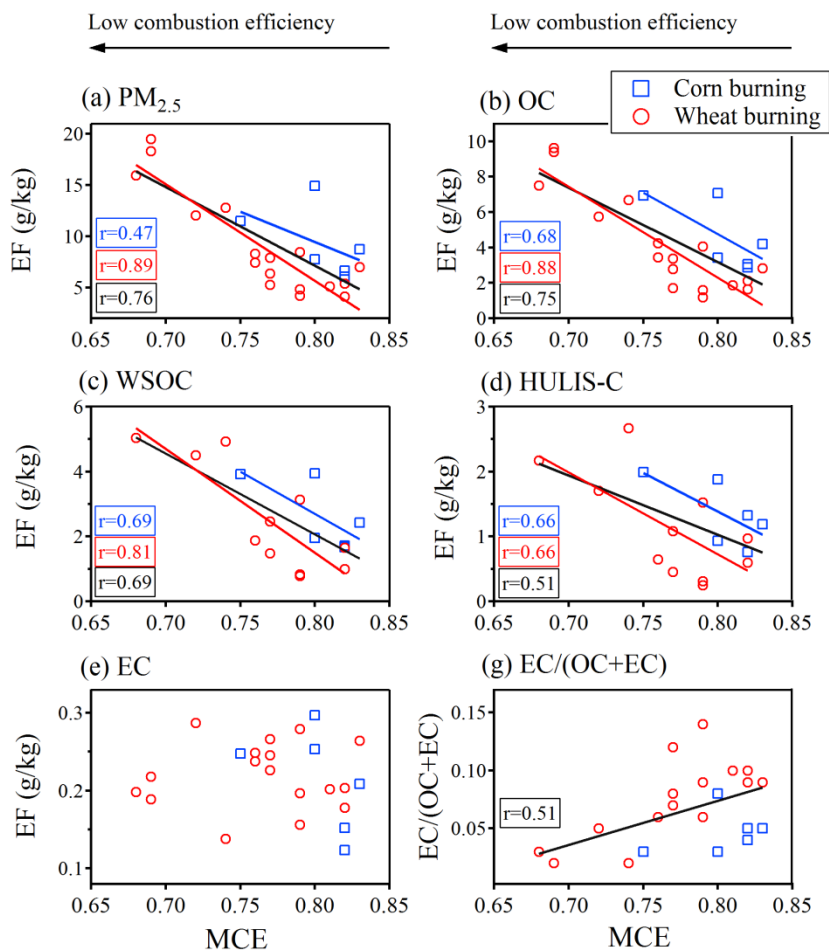


545

546 Figure 2 Emission factors of PM_{2.5}, OC, WSOC, HULIS_c and EC from (a) corn burning and (c) wheat burning, and emission
 547 factors of low molecular weight organic acids (acetic acid, formic acid, succinic acid, and oxalic acid) from (b) corn burning
 548 and (d) wheat burning. The EC emission factors are represented by 5×EC due to the low values. The pie charts in panels (a)
 549 and (c) represent the contribution of major carbonaceous aerosols among PM_{2.5}. The high-polarity WSOM (WSOM-h) is
 550 calculated by subtracting HULIS from WSOM. Different moisture content levels correspond to those shown in Table S1.



551
552

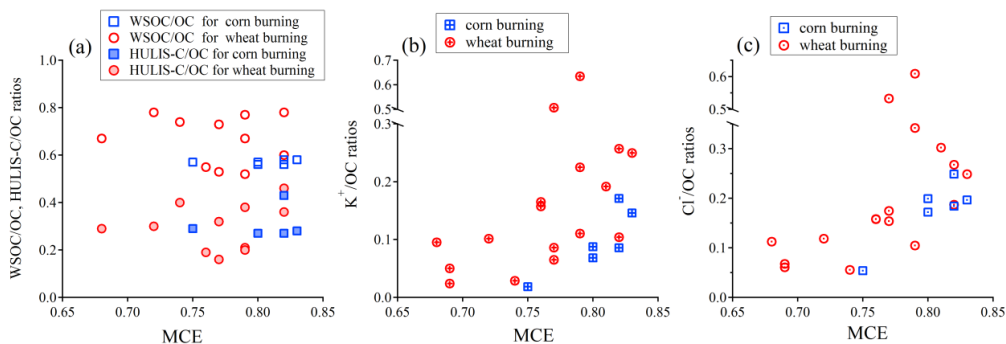


553

554 Figure 3 Emission factors of $PM_{2.5}$, carbonaceous aerosols (OC, WSOC, HULIS_C and EC) and $EC/(OC+EC)$ ratios as a
555 function of modified combustion efficiency (MCE). Corn and wheat burning emissions are denoted by red and blue colors,
556 respectively. The r values in each panel are the correlation coefficients between emission factors and MCE for corn (blue),
557 wheat (red) and the overall (black) burning experiments.

558

559



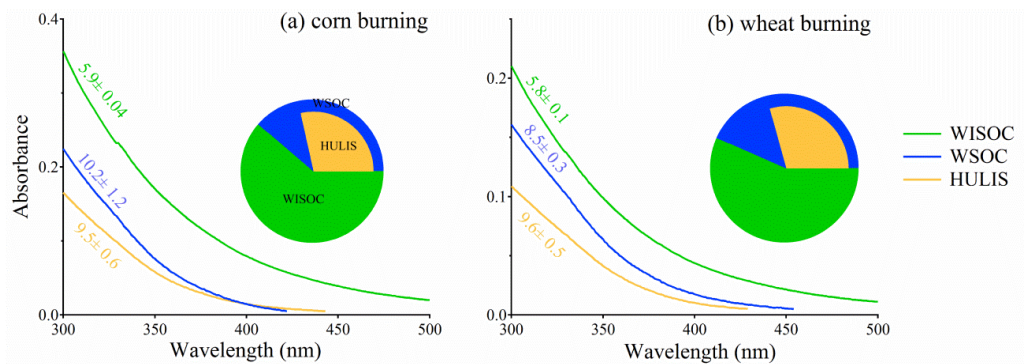
560

561 Figure 4 Variations of (a) WSOC/OC and HULIS_C/OC ratios, (b) K⁺/OC, and (c) Cl⁻/OC ratios as a function of modified
562 combustion efficiency (MCE) for corn and wheat burning experiments. Corn and wheat burning emissions are denoted by
563 red and blue colors, respectively.

564

565

566



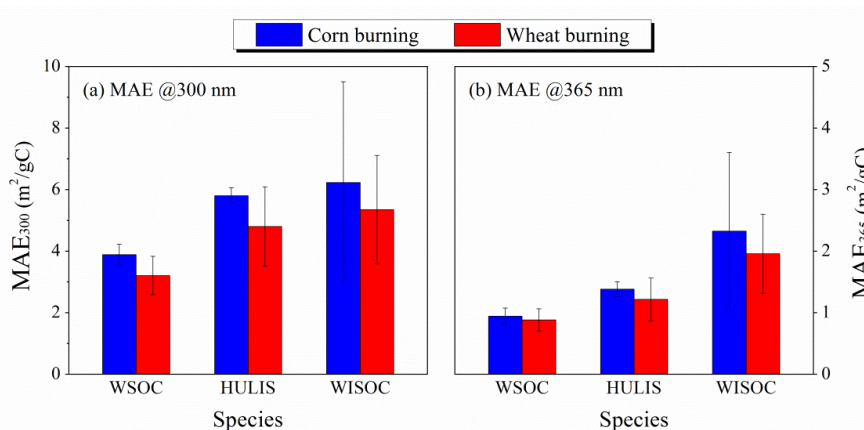
567

568 Figure 5 UV-vis spectra of carbonaceous aerosol solutions, including WSOC, HULIS_C and WISOC, from (a) corn and (b)
569 wheat burning experiments. The pie chart in each panel is the absorption contribution of different BBOA fractions at 300 nm.
570 The number represents the average AAE of each BBOA fraction derived from the absorption in the wavelength range of
571 300-450 nm.

572

573

574

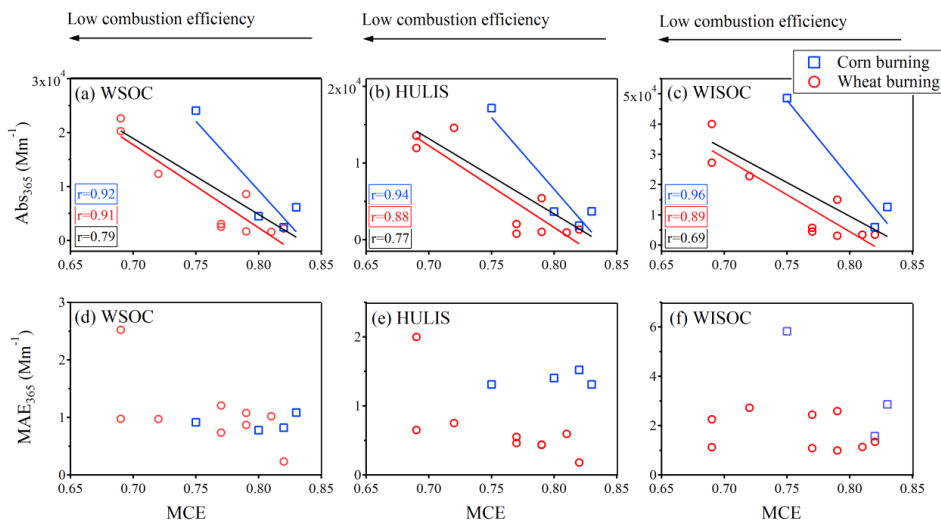


575

576 Figure 6 Mass absorption efficiency (MAE) of different organic carbonaceous aerosols, including WSOC, HULIS and
 577 WISOC emitted from corn and wheat burning.

578

579



580

581 Figure 7 (a-c) Light absorption coefficients (Abs_{365}) and (d-f) mass absorption efficiency (MAE_{365}) of WSOC, HULIS_C and
 582 WISOC at 365 nm as a function of combustion efficiency. Corn and wheat burning emissions are denoted by red and blue
 583 colors, respectively. The r values in panels (a-c) are the correlation coefficients for corn (blue), wheat (red) and overall (black)
 584 burning experiments.

585

586